Effect of electron-electron scattering on intervalley transition rates of photoexcited carriers in GaAs

M. J. Kann, A. M. Kriman, and D. K. Ferry
Center for Solid State Electronics Research, Arizona State University, Tempe, Arizona 85287-6206
(Received 7 December 1989)

The femtosecond relaxation of photoexcited carriers in GaAs is investigated by the use of ensemble Monte Carlo calculations coupled with a molecular-dynamics approach for the carrier-carrier interaction. The interaction of various scattering mechanisms and the dynamic screening of hot carriers in semiconductors is probed. At a density for which the GaAs is degenerate (in equilibrium), scattering out of the excitation volume is dominated in the initial tens of femtoseconds by electron-electron scattering, and the scattering rate increases with increasing density. This rate increase agrees both in magnitude and in its density dependence with recent experimental measurements. The presence of electron-electron scattering modifies both the population transition rates and carrier densities in the satellite valleys, primarily by reshaping the energy distribution of carriers in the central valley. Intervalley scattering rates decrease by 2 orders of magnitude as the electronic system cools during the first picosecond. Thus, intervalley processes do play a role in the initial decay and the same processes play a modified role in the picosecond-scale luminescence decay. We find that rates, for particular mechanisms of carrier transfer to the satellite valleys, must be estimated carefully since the Γ-L population shift contains a significant fraction of electrons that reach the L valleys by way of the X valleys.

I. INTRODUCTION

Advances in ultrashort-laser-pulse techniques have led to the generation of laser pulses as short as 6 fsec, which have made it possible to extend the related optical techniques into the few-femtosecond regime. These techniques have been used to measure the polarization dephasing rate, and the initial exponential decay time constant for carriers in the excitation volume (in phase space) in semiconductors.[1-6] While optical studies are of interest in their own right, it is important to note that as the dimensions of electronic devices reach the submicrometer regime, the energy and momentum losses due to carrier-carrier interactions begin to play a crucial role in device performance.[7] Carrier-carrier scattering, while conserving the total energy of the carriers, leads to evolution of the distribution function into a Fermi-Dirac-like distribution at a carrier temperature hotter than the lattice temperature.

With the current interest in ultrahigh-speed electronic and optoelectronic devices, it is important to understand the relaxation dynamics of nonequilibrium carriers in GaAs and related compounds. Ultrafast scattering and relaxation processes in semiconductor materials, which occur on a time scale comparable to the pulse duration, affect the behavior and contribute to the performance limits of electronic and optoelectronic devices. Investigations of hot-photoexcited-carrier relaxation in semiconductors have shown that a quasiequilibrium energy distribution is developed at a carrier temperature far above the lattice temperature in less than 1 psec.[7] However, the initial stages of carrier relaxation occur through an interplay of both carrier-carrier and carrier-phonon scattering, so that the understanding of the initial rapid cooling observed experimentally requires the knowledge of how this thermalization is established on the femtosecond time scale.[8,9] For this purpose, careful ensemble Monte Carlo (EMC) calculations are required. Previous EMC studies have proven to be useful in the femtosecond regime. It is known that these EMC calculations are an appropriate technique for studying transient femtosecond dynamics.[8,9]

The experimental results of Shank and collaborators,[2] who probe the fast scattering of carriers out of the central valley using pump-probe techniques with two 6-fsec pulses centered at 2 eV, show that the scattering time, which is primarily determined by scattering into both the X and L valleys, was measured to be 33 fsec for densities in the range $(3-6)\times 10^{18}$ cm^{-3}. The time resolution of the ultrashort 6-fsec laser pulse has made it possible for them to investigate directly the dynamics of intervalley scattering in GaAs. Shah's group[10] reported a slow rise of luminescence in GaAs after excitation by a subpicosecond laser pulse, due to a slow return of electrons from the L valley to the central valley. By fitting the data with an EMC calculation, they determine the Γ-L deformation potential to be $(6.5\pm 1.5)\times 10^8$ eV/cm, which confirms the measured value used here (7×10^8 eV/cm).[11] Transfer of the carriers to the satellite valleys represents a storage of energy, which is released as kinetic energy when those carriers return to the central valley. The electrons returning to the central valley act as a source of heating for the photoexcited plasma and thus slow the cooling of the electron gas.

Experiments in which faster decay rates are observed

must entail another process, such as carrier-carrier scattering. With techniques of increased time resolution, Becker *et al.*[1] report the first observation of femtosecond photon echoes from direct transitions in GaAs. The echo decay time constant was found to vary from 11 down to 3.5 fsec for carrier densities ranging from 1.5×10^{17} to 7×10^{18} cm^{-3}. This allowed them to determine the polarization dephasing rate (which is 4 times the echo decay time constant). The carrier-density dependence of the dephasing rate indicates that carrier-carrier scattering is the dominant dephasing mechanism in the rapid initial stage of relaxation and yields previously unavailable information on Coulomb screening in the nonequilibrium plasma. Collisions involving both electrons and holes can dephase the polarization of an electron-hole pair. At high carrier densities the carrier momentum loses phase coherence primarily due to the screened Coulomb interaction between carriers.

II. THE JOINT MOLECULAR-DYNAMICS–EMC METHOD

Previous studies have shown that dynamical screening effects play an important role in the short-time relaxation and must be incorporated in some way into Monte Carlo simulations.[7,12] Determining the correct screening function, however, requires a detailed specification of the carrier distribution. Determining the carrier distribution, on the other hand, is the object of EMC calculations, and the carriers are generally very energetic and far out of equilibrium. Thus, dynamical screening cannot be computed accurately before the Monte Carlo simulation is performed. This implies that the screening function should be calculated dynamically in a self-consistent way, in parallel with the Monte Carlo simulation. This can be done in effect by including the electron-electron interaction directly via a molecular-dynamics (MD) approach within the EMC technique. In this approach, the unscreened Coulomb interaction is used; screening between any particular pair of particles arises explicitly as it does in the underlying calculation of ordinary screening functions—by a deformation of the distribution of neighboring charges.

Numerical simulation of a large number of particles via MD approach is usually considered to be very computer-time intensive. This is particularly the case for a long-range *(unscreened)* Coulomb interaction. However, we have carried out calculations for 2000 particles using a vectorized program, and these calculations can be performed in reasonable time. The precision of the calculation is enhanced by having each particle interact simultaneously not only with all other particles in the simulation region, but also with all of the periodic replicas of the particles, in a manner which eliminates the artificial Fourier periodicity. This is done efficiently by means of an Ewald sum technique.[13] Furthermore, because only a limited number of carriers may be simulated, the size of the (cubic) simulation region in the real space is set by the number of particles simulated and the photoexcited electron density. Because the Ewald sum is essentially exact, dependence of simulation results on the size of the box is minimized. Details of the calculational procedure are similar to those reported previously for Si by Lugli and Ferry.[14] One reference simulation region is used, with periodic boundary conditions fixed in the "laboratory" reference frame. In addition, force calculations are performed using translates of the reference simulation region, centered on each individual particle. This latter moving reference simulation region ensures that we evaluate the net force by summing through the set of shortest equivalent particle distance vectors in the Ewald sum.

The screening arises entirely from the adiabatic deformation of the charge distribution of the conduction electrons in the fields of uniform background charges. Existing theories of screening are valid only for equilibrium carrier distributions. Currently a good theory does not exist to describe the process of dynamic screening in such highly nonequilibrium carrier distributions. Most analytical approaches with carrier-carrier scattering do not fully incorporate the energy scattering inherent in this process, or the complex far-from-equilibrium distribution functions, and are handicapped by approximations to detailed time-dependent screening. In particular, when the assumption of local equilibrium or of the adiabatic motion of the screening electrons ceases to be valid, the Thomas-Fermi screening model for the degenerate case allows no further refinement. The Debye screening model for the nondegenerate case is similarly not valid in our problem.

The Lindhardt screening formula is more general, and able to take account of deviations of the system from an equilibrium distribution. However, its evaluation requires a knowledge of the system's distribution function. In the near equilibrium case, it is possible to use the equilibrium distribution, and the deviation from equilibrium is a higher-order correction that may be ignored. Far from equilibrium, as we are in this problem, such an approach is not valid, and to use the Lindhardt formula would require a continuous updating of the distribution appearing in it. The Lindhardt formula also suffers from the drawback—again not important near equilibrium—that it is derived perturbatively. One needs some other method which treats the same problem from a dynamical point of view. By utilizing the MD approach, we thus can treat the intercarrier potentials exactly and avoid any assumptions on the form of the dielectric function which is used in the screening process.

In computing the scattering rates, we neglect degeneracy. This is justified by the highly excited state of the system, which raises the electron system into the nondegenerate regime. As a measure of this, we observe that *if* all the photogenerated electrons remained within the excitation region, then for our highest density they would represent only a 10–15 % occupancy of the states in that energy range. (This is comparable to the occupancy at $\gtrsim 2k_BT$ above the Fermi energy in equilibrium.) The electronic states into which they scatter have even lower occupancies.

In our calculations, carrier-carrier scattering does not occur as a discrete event. Rather, the molecular-dynamics simulation incorporates the carrier-carrier in-

teraction incrementally in computing the carrier paths, which allows us to study the buildup of screening dynamics directly. The present simulation incorporates only the electron-electron interaction. This is a justifiable approximation, however. Because the holes are much heavier than the electrons, and also much colder, the center-of-mass and laboratory frames for an electron-hole pair essentially coincide, and electron-hole scattering is approximately elastic. In other words, scattering from holes approximates ionized impurity scattering, so that essentially no energy exchange is involved, and contributes primarily to momentum relaxation. This was confirmed numerically in earlier work by Osman and Ferry[7] on the role of the electron-hole interaction on the picosecond time scale, which showed that the dominant part of the distribution relaxation occurs by electron-electron scattering. Electron-hole recombination is also negligible in the first picosecond after excitation, and that process is excluded from our simulations.

The neglect of electron-hole scattering is realized in our simulations simply by not including within the MD computation the electrostatic forces exerted upon the electrons by the holes. Since we are examining the electron statistics only, the MD calculation does not need to time evolve the hole positions. As discussed earlier, within the MD-EMC approach the screening is determined in the same way as the carrier-carrier scattering: both arise in a unified manner from the explicit trajectories of the charged-carrier ensemble. Thus, by excluding the electron-hole scattering we also exclude the holes' contribution to the screening function. Again because the holes are heavier, their contribution to the high-frequency screening function is small. In general, of course, hole effects cannot be ignored. In particular, momentum relaxation effects are expected to be important in high fields, where they mediate energy exchange between carriers and field. In the future, the present methods will be extended to include holes.

III. SIMULATION RESULTS

A. Initial relaxation time

We simulated the time evolution of electrons in GaAs at 300 K, excited by a 20-fsec pulse of 2-eV photons. We use masses, coupling constants, and other physical parameters[15] that have been confirmed by several measurements using a variety of techniques.[10,11] The pulse profile was rectangular (sharp on, sharp off), but for most analytical purposes this is not a severe approximation, and this process allows a more direct evaluation of scattering rates. For this photon energy, the initial electron distribution is generated from all valence bands (light, heavy, and splitoff). About 50% of the electrons are generated from the heavy-hole band. The electron population was followed in the central Γ and satellite L and X valleys. Excitation is direct only into the Γ valley, and electrons enter the satellite valleys only by subsequent phonon scattering.

A primary motivation of our study was to understand the earliest stages of optical-absorption relaxation observed in the related optical techniques (e.g., pump-probe experiments[2,6,16] or equal-pulse correlation techniques[3,4]). In the experiments, when a semiconductor is photoexcited by interband absorption of high-intensity ultrashort laser pulses, the carriers are excited into a narrow distribution of energies determined by the exciting laser's bandwidth and the band structure of the material. The well-localized distribution function immediately begins to be altered by carrier-carrier and carrier-phonon scattering. At high densities ($>10^{18}$ cm^{-3}), initial time scales are observed experimentally by Becker *et al.*[2] for this relaxation which are too short to be explained in terms of intervalley scattering.[8,17] In our simulations, the excitation region is defined to be the range of energies into which the heavy holes are photoexcited (including the correction for thermal broadening), which parallels the sample transparency.

The relaxation time of the conduction-band electrons out of the initial photoexcited states is clearly of fundamental importance because it limits the intrinsic lifetime of the corresponding Bloch states in the conduction band. It is also important for the understanding of, for example, high-speed GaAs devices and laser annealing processes. In Fig. 1, we show the population of electrons in the central valley that remain in the initial excitation volume after being excited from the heavy-hole band. The scattering out of these original optically excited states is basically dominated by a single exponential decay at very short times. The decay time constant in Fig. 1, for a density of 4×10^{18} cm^{-3}, varies from 16 to 46 fsec over the first 80 fsec following the end of the pulse (20–100 fsec), averaging about 30 fsec, which is comparable to the results measured by Rosker *et al.*[3] They obtained a fastest exponential decay time constant of about 40 fsec for carrier density of 3×10^{18} cm^{-3}. Computed from the slopes in Fig. 1 just after the laser pulse, at $t=20$ fsec, we find time constants of 56 and 33 fsec for densities of 5×10^{16} and 5×10^{17} cm^{-3}, respectively.

In Fig. 2, this single exponential time constant determined from such curves is plotted as a function of the

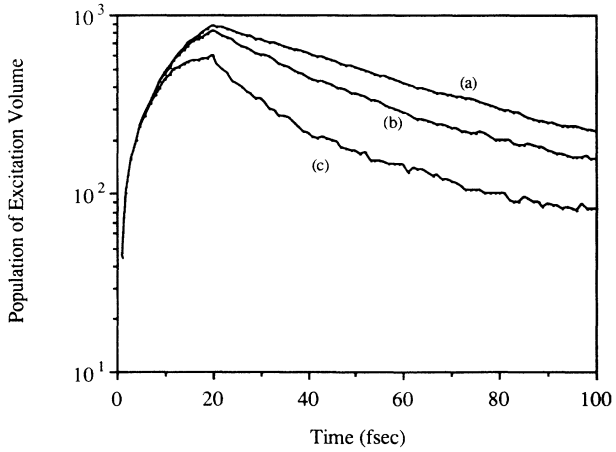

FIG. 1. Electron density in the excitation region for densities (a) 5×10^{16} cm, (b) 5×10^{17}, (c) 4×10^{18} cm^{-3}.

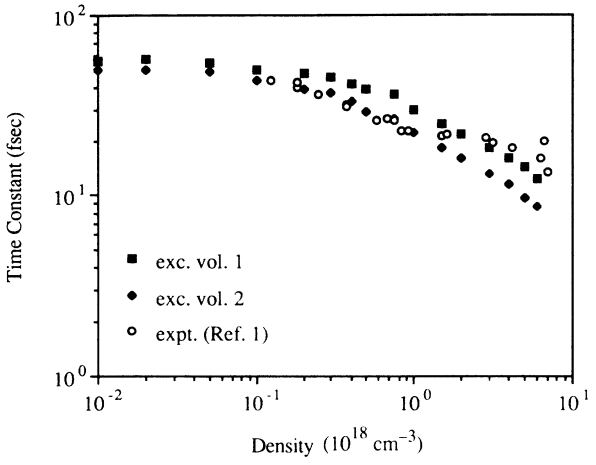

FIG. 2. The decay time constant for scattering out of the excitation volume for a 2-eV photon excitation. The decay is dominated by electron-electron scattering.

density of photoexcited carriers in a log-log form compared with the experimental polarization dephasing times obtained by Becker *et al.*[1] These experiments provide the first information on nonequilibrium screening processes on such a rapid time scale. The difference of the probing energy range (and hence, the difference in excitation "volume") between those two sets of theoretical data is just the polar optical-phonon energy, 36 meV. It is obvious that if the initial excitation volume is smaller, the relaxation rate increases, indicating the dominance of electron-electron scattering. Our results from EMC calculations agree with Becker's experimental results within a reasonable range and also give good agreement with the values cited by Tang's group[3,4] for the various time constants. The decay rate is clearly an increasing function of density, particularly in the very early times following photoexcitation. The density dependence alone suggests strongly that electron-electron scattering is the dominant mechanism for the decay. In this view, electrons leave the initial excitation region by scattering in energy to other parts of the Γ valley. However, the density dependence is weak because stronger screening at high densities partially compensates the effect of more frequent collisions.[2,8]

The systematic change in the shape of the curves (a)–(c) in Fig. 1 is also evidence for relaxation by an electron-electron scattering mechanism. The lowest-density curve is very straight on a semilog plot: it has a well-defined relaxation time. The higher-density curves are increasingly convex ("concave up"). This is consistent with depletion by a process of diffusion in energy space. In general, diffusion from an initial distribution cannot be characterized by a single lifetime. (Indeed, it follows an asymptotic inverse power law with a half-integer exponent.)[18]

The data shown in Fig. 2 suggests that there is a "knee" behavior in the time constant for decay of the number of particles in the excitation volume, which decreases rapidly with increasing density. On the log-log scale shown here, this decay is almost linear in nature for densities beyond a certain point which is already degenerate. We find the time constant is related to the carrier density in a power-law behavior which is determined from the slope. Below this point, however, the time constant does not seem to vary much with the excitation density. The decay rate becomes sufficiently slow that the intervalley scattering processes become the significant part of the total rate. In the dephasing experiments of Becker *et al.*[1], they suggest that T_m (momentum relaxation time) varies with $N^{-1/3}$ in the limit of large carrier densities which can be explained by the simple-minded Thomas-Fermi approximation. However, the Thomas-Fermi approximation is not valid in this situation because the excited carrier distribution is nonthermal. Our results do not quite support their arguments about the value of the exponent. As the dephasing time becomes comparable to the electron-phonon interaction time, phonon processes are expected to begin to dominate and the dephasing time should become independent of excitation density. Clearly, the data presented in Fig. 2 suggested that the phonon lifetime is of the order of 50 fsec. The long lifetime at low density suggests that we may have to reevaluate the lifetimes for scattering to the satellite valleys.

It should be pointed out that the measurements of Becker *et al.*[2] by pump-probe techniques using two 6-fsec laser pulses and made for a density range of $(3-6)\times 10^{18}$ cm^{-3}, exhibit a lifetime of 33 fsec and their measured lifetime was independent of the density, which does not agree with their own results of the dephasing experiments.[1] However, they fit well to the data of Tang and collaborators,[3,4] which gives 33–34 fsec at the lower end of this density range. Although the experimental techniques are different, there is still an incongruity between Becker's two results. This variation in the measurements, and with the current theory, is puzzling, and warrants further investigation.

The picture of initial relaxation by electron-electron scattering is further supported by observing the number of electrons occupying the satellite valleys (Fig. 3). While at one point, more than half of the electron population is in the satellite valleys, the time for this is reached long after the excitation region is depleted to a few percent of its initial occupation. The rate of polar-optical scattering events can be computed with greater confidence than intervalley scattering rates (if only because the electron-phonon matrix element is more accurately known), and this process also does not play an important role in the initial relaxation from the excitation region. In the pump-probe experiments, due to the large bandwidths of the ultrashort pump and probe pulses, optical-phonon emission or absorption by either electrons or holes does not make a significant contribution to the initial relaxation.

In principle, electrons might relax from the excitation region by a mechanism that involved rapid transitions into and back out of the satellite valleys. This is a possibility because the short-time transition rates need not be such as to produce a distribution exponentially weighted toward lower energies. In contrast, at long times the ap-

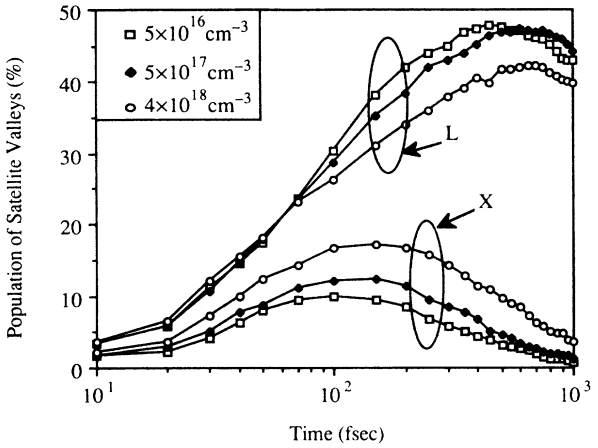

FIG. 3. Population of the satellite valleys for three densities. The upper three curves show L-valley population, the lower three show the X valley. In this and all the subsequent graphs, symbol shapes correspond to densities according to the following rule: squares, 5×10^{16} cm^{-3}; diamonds, 5×10^{17} cm^{-3}; circles, 4×10^{18} cm^{-3}.

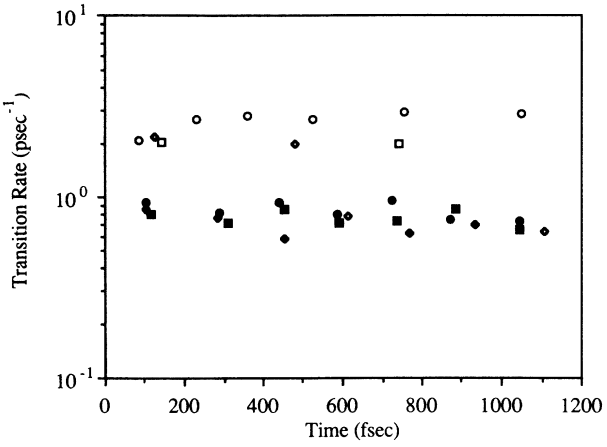

FIG. 5. Transition rates from the X and L valleys to the Γ valley. Open symbols indicate X-to-Γ rates, solid symbols the rates from L to Γ. Symbol shapes correspond to electron densities as in Fig. 3.

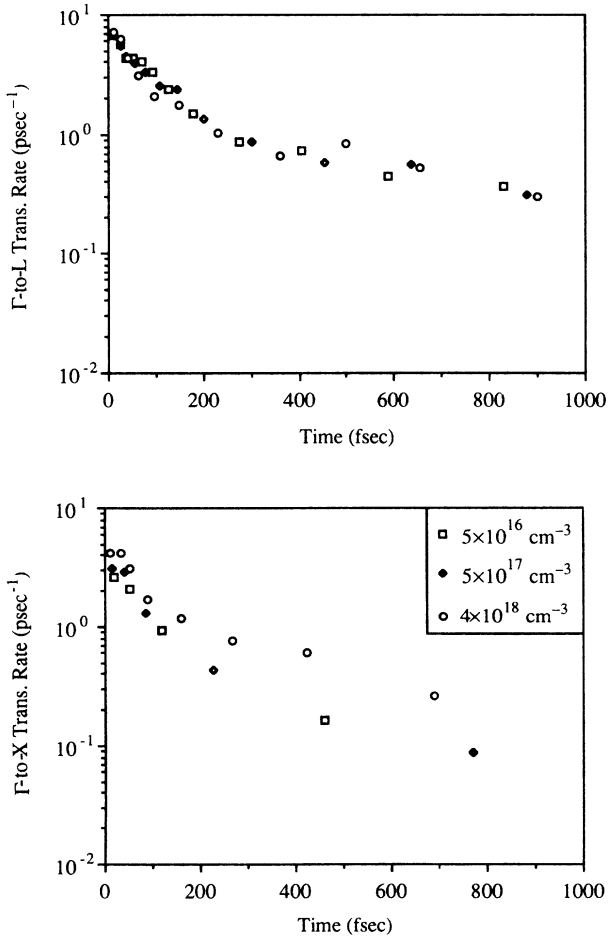

FIG. 4. Transition rates from the Γ valley to (a) the L valley and (b) the X valley, for three electron densities (legend for figure symbols applies to both graphs).

proach to a thermal distribution makes transition rates back into the Γ valley much greater than those into the higher-energy satellite valleys [see Figs. 4(a), 4(b), and 5], so the late occurrence of peaks in Fig. 3 immediately rules out intervalley scattering as a significant contributor to the initial relaxation. In the highly nonequilibrium femtosecond regime, however, it is necessary to investigate directly the rate of intervalley transitions. Our work was done in the fashion that the populations of the various valleys, and of the excitation volume, are carried out in the presence of the full set of complicated Γ-X-L processes, and electron-electron scattering, so that the population of the L valley includes electrons that have arrived there after passing through the X valley.[19] In this study, we describe the details of the electron population redistribution among different valleys, paying particular attention to those processes which are sensitive to electron-electron scattering.

B. Intervalley transition rates

As we indicated above, time-dependent transition rates may occur before thermalization. In Fig. 4(a), this is illustrated with the $\Gamma\rightarrow L$ transition rate $R_{\Gamma\rightarrow L}(t)$ for three different electron densities with the error bars omitted (errors bars are 3–5 times the symbol width). As electrons in the Γ valley cool subsequent to the initial excitation, this rate decreases monotonically. The initial decay of the transition rate may be viewed in either of two related ways. At very short times, before the electrons can thermalize within the Γ valley, the decay of the transition rate reflects depletion of *some* of the electrons in the Γ valley—those likely to scatter into the L valley (i.e., those with sufficient energy). Since these are also *depleted* primarily by means of scattering into the L valley, the slope $|\dot{R}_{\Gamma\rightarrow L}(0)/R_{\Gamma\rightarrow L}(0)|$ of the curve in Fig. 4(a) (corresponding to a time of 120±15 fsec) is comparable to the highest values of the scattering rate itself (ini-

tially, $\tau_{\Gamma\to L}=130\pm15$ fsec). Depletion by escape to the X valley also occurs, with an initial rate of $1/(350\pm30$ fsec). A Matthiessen's-rule correction then predicts an initial decay rate of $|\dot{R}_{\Gamma\to L}(0)/R_{\Gamma\to L}(0)|=1/(95\pm10$ fsec). The above numbers are for a density of 5×10^{16} cm^{-3} case. (As we shall see below, electron-electron scattering does not significantly change the number of electrons available for transfer to the L valley.)

At later times, the decay of the transition rate represents cooling of electrons in the Γ valley as a whole. The Γ valley loses energy in two ways: polar-optical-phonon (POP) scattering, and preferential transfer of the hottest electrons into satellite valleys. Since electrons just excited from the heavy-hole band typically have $\sim(10-15)\hbar\omega_0$ above the conduction-band edge, and since POP scattering occurs at a rate slower than that of intervalley scattering, intervalley transfer predominates initially. It can be seen in Fig. 3 that by about 600 fsec, the population in the satellite valleys has reached a maximum, and at the same time $R_{\Gamma\to L}$ has leveled off. At these times, the $\Gamma\to L$ rate plays an important role in luminescence decay.[10] From Fig. 3, we find that X valley population peaks around 160 fsec, which seems to agree with results inferred by Alfano and collaborators,[16] who reported evidence of the electron scattering rate to the X valley within 170 fsec by using femtosecond pump and probe absorption measurements.

Figures 4(a) and 4(b) show $R_{\Gamma\to L}$ and $R_{\Gamma\to X}$ for three simulations spanning almost two decades of density. The $\Gamma\to L$ rates show no statistically significant density dependence. This is what one would expect in a simple picture, since the absorption of a phonon by deformation potential interaction is a single-electron process. In contrast, the $\Gamma\to X$ rates show a strong density dependence. The mechanism of this effect is the electron-electron scattering in the Γ valley: The threshold for transfer into the X valley lies at the upper edge of the excitation region. Even after accounting for thermal broadening, less than one tenth of the photoexcited electrons have sufficient energy to make the transition. At high density, electron-electron scattering is increased and the energy distribution is broadened. Because electron-electron scattering preserves the total energy within the electronic system, this broadening is approximately symmetrical towards greater and smaller energies. This increases the fraction of electrons above the threshold for $\Gamma\to X$ scattering. Transitions to the L valley do not exhibit a similar effect because, for the 2-eV laser energy used, essentially all of the photoexcited electrons are above threshold. Note that, although the $\Gamma\to L$ transition rates themselves are not appreciably dependent on the density, there is some density dependence in the L valley occupancies in Fig. 3 due to the effect of $L\leftrightarrow X$ transitions discussed below (see Fig. 6). At high densities, competition from $\Gamma\to X$ processes depletes the Γ valley, so virtually unchanged $\Gamma\to L$ rates yield a lower L-valley population. Nevertheless, any density dependence in $\Gamma\to L$ rates due to increased electron density in X is too small to detect at the current level of precision. The $X\to\Gamma$ and $L\to\Gamma$ rates are in the range of $(2-3)\times10^{12}$ and $(6-10)\times10^{11}$ sec^{-1}, respectively, for three different densities (see Fig. 5). The scattering time constants are approximately 450 fsec and 1.3 ± 0.3 psec for $X\to\Gamma$ and $L\to\Gamma$ transitions, respectively.

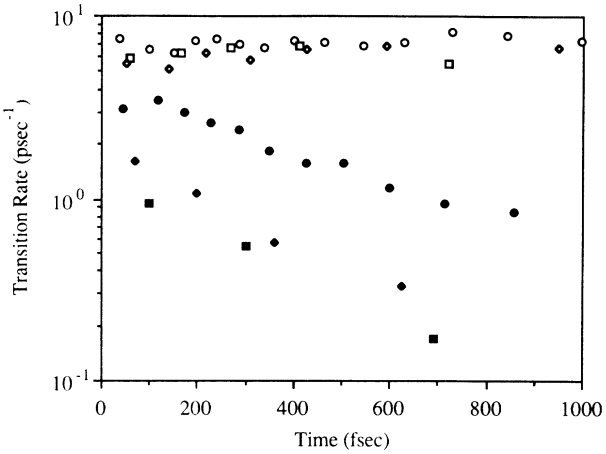

FIG. 6. Transition rates between the X valley and the L valley. Open symbols indicate X-to-L rates, solid symbols the rates from L to X. Symbol shapes correspond to electron densities as in Fig. 3.

It should be noted that electron transition rates among valleys are hard to determine just from valley population data such as that in Fig. 3. The determination of a lifetime from the population data must be done very carefully to unfold such multiple pass-through intervalley processes. This applies to both theory and experiments. For example, the long time decay of the X-valley population is plotted in Fig. 7, along with least-squares fits to exponentials with time scales of 347, 356, and 579 fsec for densities of 5×10^{16}, 5×10^{17}, and 4×10^{18} cm^{-3}, respectively. Although the fits are apparently good, these rates arise in fact primarily from a complicated reflux process involving L and Γ valleys and frequent exchange of electrons between X and L valleys. The $X\to L$ scattering time constant is about 150 fsec, independent of density

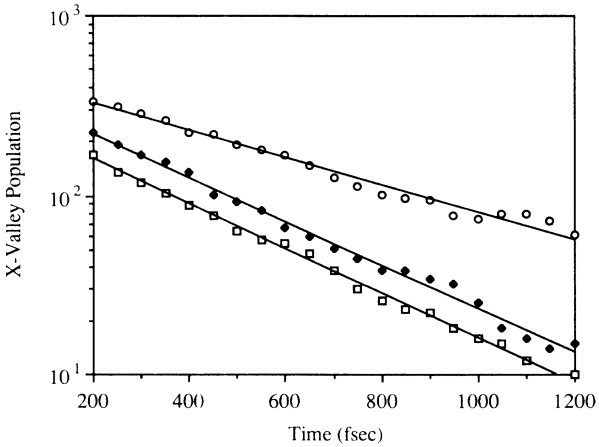

FIG. 7. Population of the X valleys. Data point symbols conform to legend in Fig. 4(b).

and time. The $L \rightarrow X$ scattering rate decreases with time, but the total rate of $L \rightarrow X$ transfer remains comparable to the $X \rightarrow L$ and $X \rightarrow \Gamma$ transfers because the L-valley population falls relatively slowly. The difference in X valley time constant between 4×10^{18} cm^{-3} and the lower densities is due primarily to increased reflux from the L valley at the higher density.

In Fig. 7, we can also see some oscillatory behavior of the X-valley population in the longer time scale, which may be related to chaotic phenomena involved in this highly nonequilibrium electron system. This could result in some further interesting investigations related to chaos in semiconductors.

IV. CONCLUSIONS

In summary, the complicated intervalley scattering rates are carefully examined here to unfold multiple pass-through processes in order to gain information on the initial stages of relaxation of the hot photoexcited carriers. We show again that electron-electron scattering is the dominant mechanism for the earliest stages of optical-absorption relaxation. We calculate the intervalley transition rates directly with the EMC process and show that some of these rates vary with time and some are sensitive to carrier density due to the effect of electron-electron scattering. The Γ-to-L rates show no statistically significant density dependence, while the Γ-to-X and L-to-X rates show a stronger density dependence. These three rates slow 2 orders of magnitude as the electronic system cools in the first picosecond. The X-to-L and X-to-Γ rates do not have statistically significant time dependences, suggesting that there is no appreciable carrier cooling within the X valley. We find that the presence of electron-electron scattering modifies the population transition rates and the satellite-valley populations.

ACKNOWLEDGMENTS

This work was supported by the Office of Naval Research. The authors are indebted to R. P. Joshi, S. M. Goodnick, P. Lugli, P. Poli, L. Rota, and J. Shah for helpful discussions.

[1]P. Becker, H. Fragnito, C. Brito Cruz, R. Fork, J. Cunningham, J. Henry, and C. Shank, Phys. Rev. Lett. **61**, 1647 (1988).

[2]P. C. Becker, H. L. Fragnito, C. H. Brito Cruz, J. Shah, R. L. Fork, J. E. Cunningham, J. E. Henry, and C. V. Shank, Appl. Phys. Lett. **53**, 2089 (1988).

[3]M. J. Rosker, F. W. Wise, and C. L. Tang, Appl. Phys. Lett. **49**, 1726 (1986).

[4]F. W. Wise, I. A. Walmsley, and C. L. Tang, Appl. Phys. Lett. **52**, 605 (1987).

[5]R. W. Schoenlein, W. Z. Lin, E. P. Ippen, and J. G. Fujimoto, Appl. Phys. Lett. **51**, 1442 (1987).

[6]W. Z. Lin, J. G. Fujimoto, E. P. Ippen, and R. A. Logan, Appl. Phys. Lett. **51**, 161 (1987).

[7]M. A. Osman and D. K. Ferry, Phys. Rev. B **36**, 6018 (1987).

[8]M. J. Kann and D. K. Ferry, in *Proceedings of the Picosecond Electronics and Optoelectronics Conference,* Salt Lake City, 1989, edited by T. C. L. Gerhard and D. M. Bloom (Optical Society of America, Washington, D.C., 1989).

[9]D. W. Baily, C. J. Stanton, M. A. Artaki, K. Hess, F. W. Wise, and C. L. Tang, Solid-State Electron. **31**, 467 (1988).

[10]J. Shah, B. Deveaud, T. C. Damen, W. T. Tsang, A. C. Gossard, and P. Lugli, Phys. Rev. Lett. **59**, 2222 (1987).

[11]K. Kash, P. A. Wolff, and W. A. Bonner, Appl. Phys. Lett. **42**, 173 (1983).

[12]S. Das Sarma, J. K. Jain, and R. Jalabert, Phys. Rev. B **37**, 6290 (1988).

[13]D. J. Adams and G. S. Dubey, J. Comput. Phys. **72**, 156 (1987).

[14]P. Lugli and D. K. Ferry, Phys. Rev. Lett. **56**, 1295 (1986).

[15]S. N. Chamoun, R. P. Joshi, E. N. Arnold, R. O. Grondin, K. E. Meyer, M. Pessot, and G. A. Mourou, J. Appl. Phys. **66**, 236 (1989).

[16]A. Katz and R. R. Alfano (unpublished).

[17]D. K. Ferry, R. P. Joshi, and M. J. Kann, in Proc. SPIE **942**, 2 (1988).

[18]T. Kurosawa, in Proceedings of the International Conference on the Physics of Semiconductors, Kyoto, 1966 [J. Phys. Soc. Jpn. Suppl. **21**, 424 (1966)].

[19]W. B. Wang, N. Ockman, M. Yan, and R. R. Alfano, Solid-State Electron. **32**, 1831 (1989).